ChemComm

Cite this: *Chem. Commun.*, 2012, **48**, 5862–5864

www.rsc.org/chemcomm

COMMUNICATION

Inside-out core–shell architecture: controllable fabrication of Cu_2O@Cu with high activity for the Sonogashira coupling reaction†

Jiahui Kou,*[a] Amit Saha,[a] Christina Bennett-Stamper[b] and Rajender S. Varma*[a]

Received 2nd March 2012, Accepted 23rd April 2012
DOI: 10.1039/c2cc31577g

Inside-out core–shell architectures (Cu_2O@Cu) with a Cu_2O core and a Cu shell, which are in contrast to the normally reported Cu_2O-outside structure (Cu@Cu_2O), were fabricated. This strategy can also be applied to construct square and hexapod Cu_2O@Cu. The obtained Cu_2O@Cu composite exhibits excellent catalytic activity for the Sonogashira coupling reactions.

As low-cost and versatile materials, Cu and its oxides have attracted great interest due to their excellent performance in the field of catalysis, superconductivity, photovoltaics, magnetic storage, electrochemistry, and biosensing.[1–7] It is well known that morphology has an important effect on both physical and chemical properties; therefore, much attention has been paid to controllable construction of materials.[8,9] Among various morphologies, core–shell structures are of significant interest owing to their unique architecture, bifunctional characteristics, and enhanced activity.[5,7,10–12] In general, sacrificial template-directed chemical transformation, based on the Kirkendall effect, is an effective approach to fabricate core–shell structures.[7,13] This method, in combination with oxidative reactions of Cu, has been widely used to generate Cu_2O-outside core–shell structure with a Cu core and a Cu_2O shell (Cu@Cu_2O).[5,7,11–15] However, in contrast to oxidation that can be easily realized by various methods, the light transition metal Cu is difficult to obtain *via* the reduction of Cu oxides in solution.[5,7,10–12] As a result, it is a challenging task to fabricate the Cu-outside structure with a Cu_2O core and a Cu shell (Cu_2O@Cu), the inside-out construction of the usually reported Cu_2O-outside Cu@Cu_2O. So far, literature reporting the successful synthesis of such a structure is very scarce, if any. Actually, in many cases Cu is expected to play a vital role as a shell because of its high activity in diverse reactions.[16] Hence, the fabrication of Cu-outside core–shell Cu_2O@Cu is extremely desirable from both an academic and a practical point of view.

Herein, we successfully develop a facile solution-phase strategy to construct the Cu-outside Cu_2O@Cu, which is the inside-out architecture of normally reported Cu@Cu_2O. By the use of the present strategy, the reduction of Cu^{2+} can take place in the mixture containing ethylene glycol and glucose at near ambient conditions, which provides excellent controllability. It is known that nonspherical core–shell structures are hard to achieve, because of the difficulties inherent in both the formation of uniform coating around high-curvature surface and the availability of nonspherical templates.[17] Besides spherical Cu_2O@Cu core–shell structures, in this study, square and hexapod structures with the same core and shell components were also successfully fabricated. This demonstrates the generality of our synthetic strategy. Moreover, the obtained Cu_2O@Cu core–shell structure exhibits excellent catalytic activity in the Sonogashira coupling reactions (Table 1). This high activity derived from the special architecture without a noble metal is fascinating; usually a noble metal is employed for such reactions.[16,18–21] This Cu_2O@Cu material may provide a promising alternative of traditional noble metals for an economic Sonogashira coupling reaction.

Fig. 1a and b shows field-emission scanning electron microscopy (FESEM) images of typical core–shell Cu_2O@Cu. The shell Cu is formed by hundreds of eggplant shaped nanoparticles (diameter of the thick end is ~100 nm and the thin end is ~30–40 nm),

Table 1 Sonogashira coupling reactions of aryl iodides with phenylacelylenes[a]

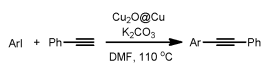

Entry	ArI	Alkyne	Time (h)	Product	Yield[b] (%)
1			8	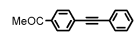	94
2			8	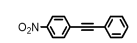	92
3			9	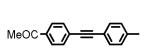	87
4			8	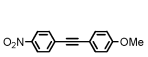	90
5			10	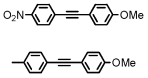	85

[a] A mixture of ArI (1 mmol), alkyne (1 mmol), Cu_2O@Cu (20 mg), K_2CO_3 (2 mmol) was heated at 110 °C in DMF (2 mL) for the required time period. [b] Yields refer to those of purified products characterized by IR and ^1H and ^{13}C NMR spectroscopic data.

[a] *Sustainable Technology Division, National Risk Management Research Laboratory, U.S. Environmental Protection Agency, 26 West Martin Luther King Drive, MS 443, Cincinnati, Ohio 45268, USA. E-mail: Varma.Rajender@epa.gov*
[b] *Water Supply Water Resources Division, National Risk Management Research Laboratory, U.S. Environmental Protection Agency, 26 West Martin Luther King Drive, MS 681, Cincinnati, Ohio 45268, USA*

† Electronic supplementary information (ESI) available. See DOI: 10.1039/c2cc31577g

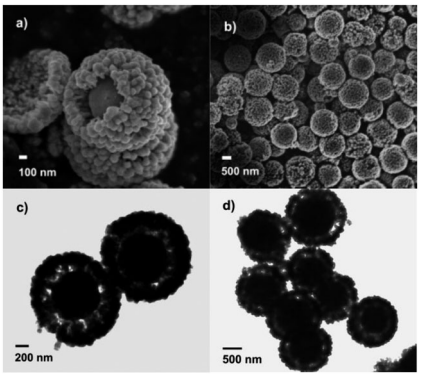

Fig. 1 Images of the typical core–shell Cu_2O@Cu. (a) High-magnification SEM image; (b) low-magnification SEM image; (c) high-magnification TEM image; (d) low-magnification TEM image.

and they are closely arrayed like broccoli (Fig. 1a). These generated core–shell Cu_2O@Cu are uniform in size and shape, according to the low-magnification SEM image (Fig. 1b). Transmission electron microscopy (TEM) images displayed in Fig. 1c and d provide insight into the morphological details of the spherical core–shell Cu_2O@Cu. The shell Cu and core Cu_2O are not completely separated from each other, but connected *via* the thin end of the nanoparticle Cu.

The experimental procedures are described in ESI.† To assess the influence of different parameters on the morphology of the Cu_2O@Cu product, a series of experiments were designed. First, the formation process of the core–shell structure was studied. As shown in Fig. 2, when the reaction time is 2 min, the surfaces of the prepared nanoparticles are smooth without small particles on them. As the time progressed, small particles began to appear on the surface and the number increased gradually. A few particles can be observed on the surface at 10 min, and then the formed particles can cover $\sim$4/5 of the surface of the microsphere at 20 min. Compact shells can be formed on the surface at 25 min and core–shell structures are thus afforded. The sizes of the cores become smaller with the extension of time; thus the cores of samples at 30 min are smaller than at 25 min. Furthermore, the cores will be completely converted to shell at 40 min, and the hollow structures are therefore obtained. Fig. 1c shows the TEM image obtained at 25 min, and other TEM images are given in Fig. S1 (ESI†), which fit well with the results from SEM. According to the pore size distribution (Fig. S2, ESI†), the average pore diameter in Cu_2O@Cu (obtained at 25 min) is about 38 nm,

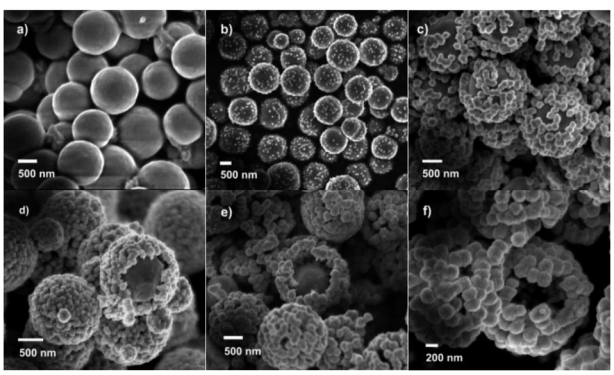

Fig. 2 SEM images of samples obtained at different time. (a) 2 min; (b) 10 min; (c) 20 min; (d) 25 min; (e) 30 min; (f) 40 min.

which is large enough for reactants and products to go through. The BET surface area is 3.7 $m^2\ g^{-1}$ for Cu_2O while 4.7 $m^2\ g^{-1}$ for Cu_2O@Cu, implying that the cover of nano Cu on the surface of Cu_2O conduce to the increase of Cu_2O@Cu surface area.

The phase and purity of the products were determined by X-ray diffraction (XRD) measurements. Fig. S3 (ESI†) shows XRD patterns of as-prepared samples obtained under different reaction time, which are consistent with the SEM images (Fig. 2). All of the diffraction peaks of the solid sphere structured samples obtained at 60 °C after 2 min can be readily indexed to a pure cubic phase of Cu_2O with a lattice constant of a = 4.267 Å. No other impurities were found in the samples. The peaks at 29.6°, 36.5°, 42.4°, 61.6° and 73.7° can be assigned to (110), (111), (200), (220), and (311) planes of the cubic Cu_2O (JCPDS No. 78-2076). Upon increasing the reaction time (60 °C, 20 min), the peaks of the Cu phase appeared due to the formation of the core–shell structure. The features at 43.2°, 50.4°, and 74.1° correspond to (111), (200), and (220) planes of cubic Cu, respectively (JCPDS No. 85-1326). The peaks of Cu increase with reaction time, and all of the peaks can be indexed to a pure Cu phase when the reaction time is 40 min, which is just shell structure (Fig. 2f). On the basis of these results, it is safe to say that the core is Cu_2O and the shell is Cu in the Cu_2O@Cu structure.

The effect of NaOH was investigated by using different amounts (0.02, 0.0375, 0.05, and 0.1 mol), and the obtained structures are shown in Fig. S4a and b (ESI†), Fig. 2e and Fig. S4c (ESI†), respectively. With 0.02 mol of NaOH, the Cu shell cannot be formed. The shell can be formed outside of the core with 0.0375 mol of NaOH, but only $\sim$2/3 of the surface of the microsphere is covered by Cu particles. The speed of the shell formation increases with NaOH amount and the core–shell structure can be formed when 0.05 mol of NaOH is introduced; on the contrary, only the shell can be generated with 0.1 mol of NaOH. As the amount of NaOH is low (0.02 mol), the Cu shell is difficult to form even by prolonging the time (60 min) or increasing the temperature (80 °C) (Fig. S5, ESI†). These results indicate that the use of NaOH does affect the reducing ability of glucose for Cu^{2+}. Comparatively, the reduction speed of Cu_2O is not as sensitive to the use of glucose as NaOH. Though the shell formation speed is lower with 0.0056 mol of glucose (Fig. S6a, ESI†) than 0.011 mol (Fig. 2e), a part of the microsphere surface is still covered by nanoparticles at 30 min with 0.0056 mol glucose. The structure obtained by using 0.022 mol of glucose is similar to that obtained by 0.011mol; core–shell structure can be formed at 30 min (Fig. S6b, ESI†).

Temperature plays a significant role in the assembly of these core–shell structures. The materials obtained at 50, 60, and 70 °C are shown in Fig. S7a (ESI†), Fig. 2e, and Fig. S7b (ESI†), respectively; the reaction becomes faster at higher temperatures. When the temperature is 70 °C, exclusively Cu shells are obtained after 30 min. In comparison, at 50 °C only some Cu nanoparticles can be generated which are not enough to form a shell. These results indicate that 60 °C is an optimal temperature for the formation of core–shell structure. The XRD patterns of samples prepared at different temperature also indicated the faster reaction speed at higher temperature (Fig. S8, ESI†).

The anion types of copper sources have no obvious influence on the construction of core–shell structure, similar structures can be generated despite that the copper source varies from $CuCl_2$

(Fig. 2e) to $Cu(CH_3COOH)_2$ (Fig. S9a, ESI†) and $CuSO_4$ (Fig. S9b, ESI†). However, when $Cu(NO_3)_2$ is used, copper particles cannot totally cover the core Cu_2O (Fig. S9c, ESI†), implying a low reaction speed in the case of NO_3^- anions.

The effect of solvent was also studied (Fig. S10, ESI†). At low ethylene glycol amounts (0 and 10 mL), the diameter of Cu particles on the surface is more than 100 nm, and cannot form a shell. When ethylene glycol amount is increased to 20 mL, the core–shell structure can be generated with an external diameter of ~1.5 μm. The diameter of the core–shell structure decreases with the ethylene glycol dose. The external diameters of obtained particles are ~800 nm with 30 mL ethylene glycol, and the structure is still core–shell (Fig. S11a, ESI†). However, in the absence of water, the particles are just hollow spheres with diameters of ~200 nm (Fig. S11b, ESI†). The results suggest that not only does the reaction become faster at higher ethylene glycol doses, but also the size of core–shell structure can be controlled to a certain range by the water and ethylene glycol ratio. The present methodology is also applied to the synthesis of nonspherical structures. As depicted in Fig. S12 (ESI†), Cu_2O particles with square and hexapod morphology are first prepared. Based on these pre-designed morphologies, Cu_2O on the outer surface can be reduced to Cu gradually by using the same method as spherical ones. The SEM and TEM images shown in Fig. S13 (ESI†) demonstrate that the Cu shell can be formed clinging to the high-curvature surfaces of the core Cu_2O, and the shape of the template Cu_2O can be well preserved. These results, in combination with the spherical data, give evidence of the generality of our strategy for the fabrication of Cu_2O@Cu core–shell structures with tunable shapes.

According to the experimental results above, a plausible synthetic mechanism of Cu_2O@Cu core–shell structure is proposed (Scheme S1, ESI†). In the ethylene glycol–water system, spherical Cu_2O particles, which subsequently act as a sacrificial template for the generation of Cu_2O@Cu, are formed immediately after glucose was added to the reaction solution. Then, the Cu_2O particles are further reduced by glucose under strongly basic conditions, and small Cu nanoparticles are produced on the surface of Cu_2O particles. The number of small Cu nanoparticles increases with the extension of time, and finally these Cu nanoparticles cover the whole surface of Cu_2O to afford the core–shell structure. Subsequently, Cu_2O can be continuously reduced until it is completely converted to Cu, and as a result hollow Cu spheres are formed as the final product. This method should belong to the template-engaged redox etching method, which is one of the most controllable approaches for the synthesis of hollow structures.[17] If the original shape of the particles is predesigned as nonspherical ones (such as square and hexapod), the corresponding Cu_2O@Cu core–shell or hollow structures can also be produced through the similar mechanism.

The obtained Cu_2O@Cu material was employed to catalyze the Sonogashira coupling reactions of aryl iodides with phenylacetylenes. It is fascinating to observe that biarylacetylenes can be produced with excellent yields (85–94%) in the absence of noble metal Pd and ligand (Table 1). Moreover, different functional groups (such as –COMe, $–NO_2$, and –OMe) are compatible with the reaction conditions. The recovered Cu_2O@Cu after reaction still can keep the core–shell structure (Fig. S14, ESI†), implying the good stability of the structure. The recovered catalyst was reused for the Sonogashira coupling reaction of entities in entry 1, Table 1 and the yield of desired product was 85%, which suggests the considerable stable activity of the material. The yield of biaryl acetylene on Cu (obtained at 40 min), Cu_2O (obtained at 2 min), the mixture of Cu and Cu_2O, cubical and hexapodal Cu_2O@Cu is 7%, 5%, 45%, 92%, and 89%, respectively. These results indicate that the Cu_2O@Cu structure is helpful to the Sonogashira coupling reaction, and core–shell materials possess similar catalytic activity in spite of different shapes. This noble metal- and ligand-free protocol for the Sonogashira coupling reaction can be a good alternative to the classical Cu–Pd catalyzed methods, thus providing an economic and sustainable pathway to biarylacetylenes.

In summary, a facile solution-phase strategy is developed to construct the Cu-outside core–shell structures (Cu_2O@Cu) with a Cu_2O core and a Cu shell, which is the inside-out architecture of usually reported Cu@Cu_2O. In addition to spherical Cu_2O@Cu core–shell structures, the successful fabrication of square and hexapod structures demonstrates the generality of our strategy. Moreover, the Cu_2O@Cu core–shell structure shows high catalytic activity in the Sonogashira coupling reactions, despite the absence of the noble metal Pd. Our strategy may open up a route for the design and synthesis of new functional materials.

Dr Jiahui Kou and Dr Amit Saha are postdoc research participants at the National Risk Management Research Laboratory, Environmental Protection Agency, administered by the Oak Ridge Institute for Science and Education (ORISE). The support from colleagues, Dr R. Venkatapathy, Mr C. Han, and Prof. D. D. Dionysiou is appreciated.

Notes and references

1 L. Lu, Y. F. Shen, X. H. Chen, L. H. Qian and K. Lu, *Science*, 2004, **304**, 422–426.
2 X.-J. Chen, V. V. Struzhkin, Y. Yu, A. F. Goncharov, C.-T. Lin, H.-k. Mao and R. J. Hemley, *Nature*, 2010, **466**, 950–953.
3 G. Li, X. Li and Z. Zhang, *Prog. Chem.*, 2011, **23**, 1644–1656.
4 Y. Chang, J. J. Teo and H. C. Zeng, *Langmuir*, 2005, **21**, 1074–1079.
5 M. Hasan, T. Chowdhury and J. F. Rohan, *J. Electrochem. Soc.*, 2010, **157**, A682–A688.
6 T. Kudernac, N. Ruangsupapichat, M. Parschau, B. Macia, N. Katsonis, S. R. Harutyunyan, K.-H. Ernst and B. L. Feringa, *Nature*, 2011, **479**, 208–211.
7 Z. Ai, L. Zhang, S. Lee and W. Ho, *J. Phys. Chem. C*, 2009, **113**, 20896–20902.
8 L. Zhang and H. Wang, *ACS Nano*, 2011, **5**, 3257–3267.
9 Y. Sui, W. Fu, Y. Zeng, H. Yang, Y. Zhang, H. Chen, Y. Li, M. Li and G. Zou, *Angew. Chem., Int. Ed.*, 2010, **49**, 4282–4285.
10 K. P. Rice, E. J. Walker, Jr., M. P. Stoykovich and A. E. Saunders, *J. Phys. Chem. C*, 2011, **115**, 1793–1799.
11 A. Radi, D. Pradhan, Y. Sohn and K. T. Leung, *ACS Nano*, 2010, **4**, 1553–1560.
12 D. B. Pedersen, S. Wang and S. H. Liang, *J. Phys. Chem. C*, 2008, **112**, 8819–8826.
13 L. Cao, Z. Li, X. Hao, Y. Zhang and W. Wang, *J. Alloys Compd.*, 2009, **475**, 600–607.
14 T. Ghodselahi, M. A. Vesaghi and A. Shafiekhani, *J. Phys. D*, 2009, **42**, 015308.
15 T. Ghodselahi, M. A. Vesaghi, A. Shafiekhani, A. Baghizadeh and M. Lameii, *Appl. Surf. Sci.*, 2008, **255**, 2730–2734.
16 R. Chinchilla and C. Najera, *Chem. Rev.*, 2007, **107**, 874–922.
17 Z. Wang, D. Luan, C. M. Li, F. Su, S. Madhavi, F. Y. C. Boey and X. W. Lou, *J. Am. Chem. Soc.*, 2010, **132**, 16271–16277.
18 H. Doucet and J.-C. Hierso, *Angew. Chem., Int. Ed.*, 2007, **46**, 834–871.
19 E. Negishi and L. Anastasia, *Chem. Rev.*, 2003, **103**, 1979–2017.
20 G. Kyriakou, S. K. Beaumont, S. M. Humphrey, C. Antonetti and R. M. Lambert, *ChemCatChem*, 2010, **2**, 1444–1449.
21 A. Corma, R. Juarez, M. Boronat, F. Sanchez, M. Iglesias and H. Garcia, *Chem. Commun.*, 2011, **47**, 1446–1448.

